

Quantum corrections to domain walls in a model (one-dimensional) ferroelectric*

A. R. Bishop,[†] E. Domany, and J. A. Krumhansl

Laboratory of Atomic and Solid State Physics, Cornell University, Ithaca, New York 14853

(Received 29 March 1976)

A one-dimensional model Hamiltonian is considered, representative, for example, of a displacive unstable lattice ferroelectric. Krumhansl and Schrieffer have shown previously that domain-wall displacement patterns arise in a classical analysis, as a consequence of inherent nonlinearity. Using a simple variational method, a quantum description of these walls (both stationary and moving) is given, and it is shown that their appearance as elementary excitations in the system survives the passage from classical to quantum mechanics.

I. INTRODUCTION

The properties of highly anharmonic physical systems have recently been subject to considerable renewed theoretical interest. In particular, the problem of a linear chain of atoms, each in an anharmonic "on-site" potential and interacting through nearest-neighbor harmonic forces, has been treated by Krumhansl and Schrieffer¹ (hereafter KS) as a simplified model unstable lattice ferroelectric. The Hamiltonian describing this system is

$$\mathcal{H} = \sum_i \left[\frac{p_i^2}{2m} + \frac{1}{2} A u_i^2 + \frac{1}{4} B u_i^4 + C (u_{i+1} - u_i)^2 \right], \quad (1)$$

where i denotes position along the chain, and u_i is the displacement of particle i from its lattice site. This Hamiltonian is the discretized version of the one-dimensional ϕ^4 field theory of current interest,² and may be considered generally as a Ginzburg-Landau expansion for a one-component order-parameter situation.

KS and others have called attention to characteristically nonlinear solutions of the classical equations of motion for this system.³ The solutions they discussed are moving "domain walls." They were able to work out the statistical mechanics of this model using a classical functional-integral method, and found the results to be in substantial agreement with a phenomenological derivation based on a picture of independent phonons and domain-wall (solitary wave³) gases. The domain walls give rise to equally distinctive physical characteristics, including the phenomenon of a "central peak" in the one-dimensional model's structure factor, as has been observed in computer simulations.⁴ The extent to which these ideas apply in higher dimensions is as yet uncertain, however there remains the possibility that the central peaks observed in real ferroelectrics⁵ may be attributed (at least in some cases) to the appearance and dynamics of microdomain patterns.

It is, then, of interest to investigate the Hamil-

tonian (1) in a quantum-mechanical context. Since the low-temperature limit is essential in the KS procedure, it is important to establish that the domain-wall solutions to the classical equations of motion have an analog within the quantum eigenstates of Eq. (1). In previous work⁶ we considered a variational description of the static walls in the quantum version of Eq. (1) corresponding to the order-disorder limit.¹ For that case, analogy with a two-state spin system was possible, but this mapping is no longer available in the displacive limit $C \gg |A|$, when thick walls are expected.¹ In the present work, we will be concerned primarily with the displacive limit. We have considered Eq. (1) as a nonrelativistic quantum Hamiltonian and obtained an approximation for the spectrum and eigenstates corresponding to a quantum generalization of the *moving* classical domain walls.

In Sec. II we introduce a simple variational method to construct a static domain wall. States describing a moving wall are constructed in Sec. III and the expectation value of \mathcal{H} in these states is interpreted as an approximation to the moving-wall eigenvalues. The moving quantum wall is compared with its classical analog in Sec. IV, and Sec. V contains a discussion and summary.

II. STATIC QUANTUM DOMAIN WALL

For $A < 0$ the on-site part of \mathcal{H} is a double-well potential, and the ground state of the system is assumed to be doubly degenerate. We construct a Hartree-type approximate eigenstate by

$$\Psi = \prod_i \phi_i[\alpha_i(u_i - R_i)], \quad (2)$$

$$\phi_i = (\alpha_i^2/\pi)^{1/4} e^{-\alpha_i^2(u_i - R_i)^2/2},$$

where α_i and R_i are variational parameters and we have introduced normalized Gaussians as trial wave functions. The expectation value of \mathcal{H} is found after some calculation to be

$$\langle \Psi | \mathcal{H} | \Psi \rangle = E(\alpha_i, R_i) = E_R(R) + E_{\alpha R}(\alpha, R) + E_\alpha(\alpha), \quad (3)$$

where

$$E_R(R) = \sum_i \left[\frac{1}{2} A R_i^2 + \frac{1}{4} B R_i^4 + C(R_{i+1} - R_i)^2 \right], \quad (4)$$

$$E_{\alpha R}(\alpha, R) = \sum_i \frac{3}{4} B R_i^2 \alpha_i^{-2}, \quad (5)$$

$$E_\alpha(\alpha) = \sum_i \left[(\hbar^2/4m) \alpha_i^2 + \frac{1}{2} (A + 2C) \alpha_i^{-2} + \frac{3}{16} B \alpha_i^{-4} \right]. \quad (6)$$

In general we can now proceed to minimize $\langle \Psi | \mathcal{H} | \Psi \rangle$ with respect to the variational parameters $\{\alpha_i, R_i\}$. However, for extended wall patterns, continuumization is a good approximation and Euler-Lagrange minimization is possible (cf. Refs. 1 and 6). In this way we find the following coupled equations for $R(x)$ and $\alpha(x)$ ($\sum_i \rightarrow \int dx$, with unit lattice spacing):

$$2 \frac{C}{|A|} \frac{d^2 r}{dx^2} = r^3 + r \left(\frac{3}{2} \beta^2 - 1 \right), \quad (7)$$

$$\epsilon = \frac{3}{4} \beta^6 + \beta^4 (2C/|A| + \frac{3}{2} r^2 - 1). \quad (8)$$

Here we have introduced the notation $\beta \equiv (\alpha R_0)^{-1}$, $r = R/R_0$, $R_0 = (|A|/B)^{1/2}$, and

$$\epsilon = \frac{B^2 \hbar^2}{A^3 2m} = \frac{1}{4} \frac{\hbar^2}{2m R_0^2 |V_0|}. \quad (9)$$

$|V_0| \equiv \frac{1}{4} A^2/B$ is the well depth and $\pm R_0$ are the equilibrium displacements in the classical KS calculation. The displacive limit emphasized by KS is $C \gg |A|$ and in this case our continuumization is valid.

The quantum correction factor ϵ in (9) is characteristic of the Hamiltonian (1) and has the expected form of a de Boer factor (squared)—precisely this factor occurred in our analysis of the order-disorder limit.⁶ If $\epsilon = 0$ then the classical KS result is recovered: from (8), $\beta(x) = 0$, corresponding to pure δ -function trial wave functions, and then (7) becomes the nonlinear equation deduced by KS to describe their *classical, stationary* domain wall:

$$r_{cl}(x) = \tanh[(|A|/C)^{1/2} \frac{1}{2} x]. \quad (10)$$

For finite ϵ an analogous domain wall is possible with some modified characteristics. The ground state is parametrized by r_∞ , β_∞ determined as solutions of

$$\begin{aligned} \beta_\infty^6 - \frac{4}{3} (C/|A| + \frac{1}{4}) \beta_\infty^4 + \frac{2}{3} \epsilon &= 0, \\ r_\infty^2 &= 1 - \frac{3}{2} \beta_\infty^2. \end{aligned} \quad (11)$$

Using the solutions of (11) (see Fig. 1) as initial

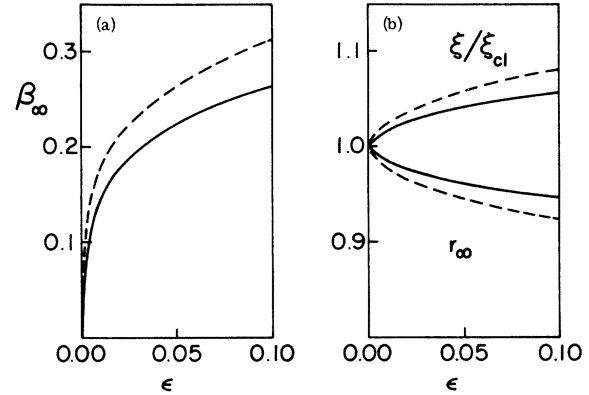


FIG. 1. (a) Asymptotic variance (β_∞) of Gaussian single-particle wave function as a function of quantum parameter ϵ . and for $C/|A| = 5.0$ (dashed line) and 10.0 (solid line). (b) Asymptotic position of the wave-function center $r_\infty \equiv (1 - \frac{3}{2} \beta_\infty^2)^{1/2}$ and wall width $[\xi/\xi_{cl} \propto r_\infty^{-1}]$; see Eq. (15). Same parameters as (a).

conditions we have solved (7) and (8) numerically.⁷ The domain patterns are compared in Fig. 2 for $\epsilon = 0$ and 0.1 and $C/|A| = 10$. However, the basic features can be easily deduced: from (8) we see $\beta(x)^4 \approx \epsilon [2C/|A| - 1 + \frac{3}{2} r(x)^2]^{-1}$ for small ϵ , so that $\beta(x)$ increases (the wave functions spread out) as $|r(x)|$ decreases, i.e., as the wall center is approached. It then follows from a simple scaling argument in Eq. (7) that the local wall gradient decreases on approaching the wall center, and the wall width increases with increasing ϵ [see Fig. 1(b)]: $r(x) \approx a^{1/2}(x) \tanh[x/\xi(x)]$, $a(x) = 1 - \frac{3}{2} \beta^2(x)$,

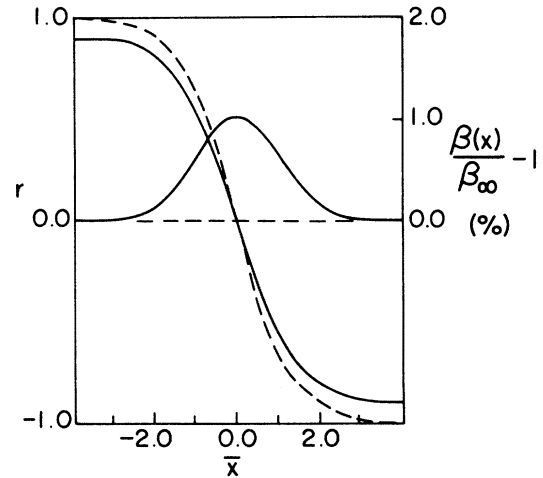


FIG. 2. Variations of the center [$r(x)$] and variance [$\beta(x)$] of the Gaussian trial wave function for a domain wall, in the classical limit (dashed lines) and with $\epsilon = 0.1$ (solid lines). The chain coordinate is $\bar{x} \equiv x(|A|/2C)^{1/2}$, and $C/|A| = 10.0$ on both cases. Note the coupling between $r(x)$ and $\beta(x)$ in the quantum case (see Sec. II).

$\xi^2(x) = 4(C/|A|)a^{-1}(x)$. These effects are small for $\epsilon \ll 1$ and $C \gg |A|$.

III. MOVING QUANTUM DOMAIN WALLS

The classical domain walls move according to a "relativistic" prescription^{1,8}: the wall width d is Lorentz contracted as $d(v) = d(0)(1 - v^2/v_0^2)^{1/2}$ and the harmonic sound speed $v_0 \equiv (2C/m)^{1/2}$ acts as a limiting wall speed (playing the role of the speed of light). Similarly, the classical wall energy is given in the continuum limit by⁸

$$\begin{aligned} E_{\text{cl}}(v) &= E_{\text{cl}}(0)(1 - v^2/v_0^2)^{-1/2}, \\ E_{\text{cl}}(0) &= \frac{1}{3}(C/|A|)^{1/2}|V_0|. \end{aligned} \quad (12)$$

We will investigate the basic features of a quantum analog of this behavior by studying

$$\Psi_q = N^{-1/2} \sum_a e^{-iqa} \Psi_a, \quad (13)$$

where

$$\Psi_a = \prod_i \phi_i[\alpha_i(u_i - R_{i-a})]. \quad (14)$$

Ψ_a describes a wall centered on site a . In the following we will take α_i as the constant α_∞ given by (11), and allow only R to vary from site to site. This assumption is made for computational convenience and can be improved, but from Sec. II the variations in α are small for small ϵ . In this approximation the continuum⁹ wall solution is found from (7) to be

$$r(x) = r_\infty \tanh(x/\xi), \quad \xi = (2/r_\infty)(C/|A|)^{1/2}. \quad (15)$$

$$\begin{aligned} \langle \Psi_q | \mathcal{H} | \Psi_{q'} \rangle &= \sum_a e^{-iq'a - \alpha_\infty^2 I_1(a)/4} \left((\hbar^2 \alpha_\infty^2 / 4m) [N - \frac{1}{2} \alpha_\infty^2 I_1(a)] + \frac{1}{2} A [NR_\infty^2 - \frac{1}{4} I_2(a) + \frac{1}{2} N \alpha_\infty^{-2}] \right. \\ &\quad \left. + \frac{1}{4} B [NR_\infty^4 - \frac{1}{16} I_3(a) + 3\alpha_\infty^{-2} [NR_\infty^2 - \frac{1}{4} I_2(a)] + \frac{3}{4} N \alpha_\infty^{-4}] + C [N \alpha_\infty^{-2} + I_4(a)] \right), \end{aligned} \quad (19)$$

where

$$\begin{aligned} I_1(a) &= \sum_i (R_i - R_{i+a})^2, \\ I_2 &= \frac{1}{4} \sum_i [R_\infty^2 - \frac{1}{2} (R_i + R_{i+a})^2], \\ I_3 &= \frac{1}{16} \sum_i [R_\infty^4 - \frac{1}{2} (R_i + R_{i+a})^4], \\ I_4 &= \frac{1}{4} \sum_i (R_i + R_{i+a} - R_{i-1} - R_{i-1+a})^2. \end{aligned} \quad (20)$$

The sums in (20) have been defined in convergent form, so that the only divergent terms in (19) are proportional to N and are a independent after normalizing according to (18). These terms correspond to the ground-state energy in the absence of a wall. Henceforth we will take $E(q)$ to be the

We proceed to calculate the energy $E(q)$ of a moving wall according to

$$E(q) = \langle \Psi_q | \mathcal{H} | \Psi_q \rangle / \langle \Psi_q | \Psi_q \rangle, \quad (16)$$

where Ψ_q is defined in terms of the variational solutions deduced in Sec. II. A rigorous variational approximation would be to minimize $E(q)$ in (16) and deduce $\{R_i(q)\}$ —the resultant wall shape would then be a function of q to be compared with the classical Lorentz contraction. We leave this full variation for future work and content ourselves here with the partial scheme above, which will be reasonable for small q . Thus the domain-wall shape remains fixed by (15) in the continuum approximation but we will find a q -dependent energy to be compared with the classical result (12).

We note in passing that the Hamiltonian (1) is translationally invariant, i.e., under the transformation $u_i \rightarrow u_{i+a}$. (The labels l , *not* the dynamic variables u_i , are translated.) Thus we can expect the eigenstates of (1) to transform as

$$\Psi_k[u_{i+a}] = e^{ika} \Psi_k[u_i]. \quad (17)$$

Although the approximate eigenstate constructed in Sec. II does not possess this property, Ψ_q of Eq. (13) does.

Calculation of the various matrix elements in (16) is laborious but straightforward. The normalization is found to be

$$\langle \Psi_q | \Psi_{q'} \rangle = \delta(q - q') \sum_a e^{-iq'a - \alpha_\infty^2 I_1(a)/4} \quad (18)$$

and

normal-ordered form of (19), corresponding to the excess energy localized in a single wall. Thus

$$E(q) = \sum_a e^{-iq'a - \alpha_\infty^2 I_1(a)/4} F(a) / \sum_a e^{-iq'a - \alpha_\infty^2 I_1(a)/4} \quad (21)$$

with¹⁰

$$\begin{aligned} F(a) &= -(\hbar^2 \alpha_\infty^4 / 8m) I_1(a) + \frac{1}{8} A |I_2(a) - \frac{1}{64} B I_3(a) \\ &\quad - \frac{3}{16} B \alpha_\infty^{-2} I_2(a) + C I_4(a). \end{aligned} \quad (22)$$

We will examine the quantum corrections contained in (21) and (22) in Sec. IV, but we can note immediately that $I_1(a)$ and $F(a)$ are even in a , so that $dE(q)/dq \rightarrow 0$, as $q \rightarrow 0$. Thus, as for the classical case, $E(q)$ has no term linear in q . It is also instructive to represent $E(q)$ in terms of aver-

ages with respect to the distribution function defined by

$$\langle O \rangle \equiv \sum_a e^{-\alpha_\infty^2 I_1(a)/4} O(a) / \sum_a e^{-\alpha_\infty^2 I_1(a)/4}. \quad (23)$$

After a little algebra we find

$$E(q) = \langle F(a) \rangle - q^2 \langle (a^2 - \langle a^2 \rangle) [F(a) - \langle F(a) \rangle] \rangle + O(q^4). \quad (24)$$

We will see in Sec. IV that, for small a , $F(a) \approx F(0) + F_1 a^2$, with $F_1 < 0$. Hence, since small a dominates the average (23), the coefficient in q^2 in Eq. (24) is positive, as for the classical result (12).

IV. QUANTUM CORRECTIONS AND THE CLASSICAL LIMIT

For comparative and numerical convenience we rewrite (22) as

$$F(a)/|V_0| = -\epsilon \beta_\infty^4 R_0^{-2} I_1(a) + \frac{1}{2} (1 - \frac{3}{2} \beta_\infty^2) R_0^{-2} I_2(a) - \frac{1}{16} R_0^{-4} I_3(a) + 4(C/|A|) R_0^{-2} I_4(a). \quad (25)$$

We recall from Sec. II that the classical limit corresponds to $\epsilon \rightarrow 0$ and $\beta_\infty \rightarrow 0$, but from (11) we deduce that $\epsilon \beta_\infty^4$ approaches a finite value:

$$\epsilon \beta_\infty^4 \xrightarrow{\beta_\infty \rightarrow 0} 2C/|A| + \frac{1}{2}. \quad (26)$$

The I sums (20) are readily evaluated. In particular, in the continuum approximation, using (15), we find that for small a (i.e., a few lattice spacings)

$$I_1(a) \simeq \frac{4}{3} r_\infty^2 R_0^2 a^2 \xi^{-1}, \quad I_2(a) \simeq 8 r_\infty^2 R_0^2 \xi, \quad (27)$$

$$I_3(a) \simeq \frac{128}{3} r_\infty^4 R_0^4 \xi, \quad I_4(a) \simeq I_1(1) \simeq \frac{4}{3} r_\infty^2 R_0^2 \xi^{-1},$$

where ξ is defined in Eq. (15). Inserting (27) into (25) yields

$$F(a)/|V_0| = F(0)/|V_0| - \frac{2}{3} \epsilon \beta_\infty^4 r_\infty^2 (|A|/C)^{1/2} a^2, \quad (28)$$

with

$$F(0)/|V_0| = 8(C/|A|)^{1/2} r_\infty (1 - \frac{1}{3} r_\infty^2 - \frac{3}{2} \beta_\infty^2). \quad (29)$$

If a is treated as a discrete variable we see immediately from Eq. (21) that only the low- a terms contribute significantly when $\alpha_\infty \gg 1$ (following from $\epsilon \ll 1$). If only the $a=0$ and $a=1$ terms in (21) are retained we find

$$E(q) = F(0) - 2[F(0) - F(1)] e^{-\alpha_\infty^2 I_1(1)/4} + q^2 [F(0) - F(1)] e^{-\alpha_\infty^2 I_1(1)/4} + O(q^4). \quad (30)$$

In the classical limit the *stationary* wall energy agrees with that found elsewhere⁸: Eqs. (30), (25), and (20) give

$$E(0) \xrightarrow{\alpha_\infty \rightarrow \infty} \sum_i [\frac{1}{2} |A| R_0^2 (1 - r_i^2) - \frac{1}{4} B R_0^4 (1 - r_i^4) + C R_0^2 (r_i - r_{i-1})^2] \longrightarrow \frac{16}{3} (C/|A|)^{1/2} |V_0|, \quad (31)$$

where the last line follows from continuumizing in i [see (29)]. However, the classical limit of a *moving* wall is more subtle, because it is evident from (30) that the exponential terms are dominant and in the classical limit, $\alpha \rightarrow \infty$, no q -dependence survives. This problem would also occur in the classical limit of any Wannier-like current representation: the wave functions are completely localized and the overlap between two distinct sites is therefore identically zero. The malady is remedied by examining (13) *after continuumizing in a* , as follows.

Equations (27) and (21) imply $E(q) = E_0 + E_1$, where E_0 is given by the first term of Eq. (30) and

$$E_1 = -|V_0| \epsilon \beta_\infty^4 R_0^{-2} I_1' \frac{\int_0^\infty da \cos qa e^{-\alpha_\infty^2 I_1' a^2/4} a^2}{\int_0^\infty da \cos qa e^{-\alpha_\infty^2 I_1' a^2/4}}, \quad (32)$$

with $I_1' = I_1(a) a^{-2} \neq f(a)$. The integrals in Eq. (32) can be evaluated in terms of Hermite polynomials¹¹—the troublesome exponentials cancel exactly and the result is

$$E_1/|V_0| = -2\epsilon \beta_\infty^2 + 4R_0^2 (\epsilon/I_1') q^2. \quad (33)$$

In view of Eq. (26), the first term of Eq. (33) vanishes in the classical limit and we are left with

$$E_1 \rightarrow \hbar^2 q^2 / 2mI_1'. \quad (34)$$

We now identify velocity with

$$v \equiv \hbar^{-1} \frac{dE(q)}{dq}, \quad (35)$$

where $E_1 \rightarrow \frac{1}{2} m I_1' v^2 - \frac{1}{3} m R_0^2 (|A|/C)^{1/2} v^2$. It is now straightforward to check that the classical result (12) is exactly recovered [to the order allowed by (27)]: $E(v) = E_{cl}(0) (1 + \frac{1}{2} v^2/v_0^2)$. If the classical limit is not taken in this continuum result we find

$$E(v)/|V_0| = 4(C/|A|)^{1/2} r_\infty (\frac{4}{3} - 2\beta_\infty^2) - 2\beta_\infty^2 (2C/|A| + \frac{1}{2} - \frac{3}{2} \beta_\infty^2) + \frac{1}{2} v^2 [\frac{2}{3} (m R_0^2 / |V_0|) (|A|/C)^{1/2} r_\infty^3] \equiv [E(0)/|V_0|] (1 + \frac{1}{2} v^2/v_0^2) \quad (36)$$

with

$$v_0^2 = v_0^2 [E(0)/E_{cl}(0)] r_\infty^{-3}. \quad (37)$$

The result (36) should be compared with the discrete- a expression (30).

TABLE I. Quantum renormalization of the wall rest mass and kinetic energy for various strengths of quantum parameter (ϵ) and intersite coupling (C).

ϵ	$C/ A $	$E(0)/E(0)_{cl}$ ^a	v'_0/v_0 ^a
0.01	10	0.89	1.03
0.01	100	0.87	1.07
0.1	10	0.68	1.12

^aEvaluated in the continuum- a approximation (see Sec. IV).

The quantum corrections are compared numerically in Table I. In view of the very approximate nature of the variational calculation the quantitative results should probably not be taken too seriously. However, the *qualitative* trends indicate that an increased quantum parameter ϵ leads to lower potential (rest) wall energy and wall effective mass¹ (kinetic energy). Furthermore, these quantum effects are greater in more displacive cases (i.e., larger values of $C/|A|$). Note that (for the parameter values in Table I) most of the wall energy renormalization can be attributed to changing the *rest* wall energy, so that the approximations introduced in Sec. III are relatively unimportant.

V. CONCLUSION

In the preceding sections we have seen how the quantum analog of the classical domain-wall solution for the ϕ^4 Hamiltonian can be generated within a variational approximation. Both the stationary and moving walls were found and it was shown how the classical limit could be recovered—requiring some care for the dynamic case (Sec. IV).

However our major theoretical conclusion from this work is that the concept of a solitary wave as an elementary excitation (KS) appears to survive the passage from classical to quantum mechanics.

In so far as these walls correspond to simple model ferroelectric domain walls, it should be appreciated that the wall motion deduced here corresponds to the ideal ballistic limit. It omits any interactions with other excitations (cf. Ref. 8) or pinning effects of impurities, dislocations, grain boundaries, surfaces, etc., which are undoubtedly important in real materials.¹² Furthermore, the quantum effect discussed here is only one of several aspects. Thus, correlation functions might be limited in the true ground state; indeed quantum critical fluctuations may completely suppress an exact phase transition.¹³ We defer consideration of these questions to future work. Again, there has been much discussion, particularly in the field theory literature,² of the renormalization of the classical domain energy by dressing with quantized small (linear) perturbations—corresponding to quantization of the particlelike solutions. In fact for the quantum sine-Gordon problem¹⁴ even the (soliton) bound-state solutions (“breathers”) are now known exactly, both for a discrete lattice¹⁵ and the continuum limit.¹⁴

In the variational calculations reported here very simple Gaussian trial wave functions were chosen to demonstrate quantum corrections qualitatively. The main numerical conclusions (Sec. IV) were that the quantum effects lower the domain wall rest mass and kinetic energy (for a given velocity), especially for thick walls. For the thick walls and relatively large quantum factors considered in Table I, the quantum corrections to the wall energy greatly exceed the barrier to wall motion from the lattice discreteness.^{8,16} For sufficiently small ϵ and $C/|A|$ these energies could be comparable, and a more careful minimization [e.g., in Eqs. (3) and (16)] will be necessary.

We have greatly benefitted from the advice of M. Peskin, and the computing assistance of J. F. Currie.

*Work supported in part by the Energy Research and Development Administration, under Contract No. E(11-1)-3161, Technical Report Number C00-3161-41.

†Present address: Physics Department, Queen Mary College, Mile End Road, London E1 4NS, U.K.

¹J. A. Krumhansl and J. R. Schrieffer, Phys. Rev. B **11**, 3535 (1975).

²For example, R. F. Dashen, B. Hasslacher and A. Neveu, Phys. Rev. D **10**, 4130 (1974); J. Goldstone and R. Jackiw, *ibid.* **11**, 1486 (1975).

³See A. C. Scott, F. Y. F. Chu, and D. W. McLaughlin, Proc. IEEE **61**, 1443 (1973); D. W. McLaughlin, J. Math. Phys. **16**, 96 (1975).

⁴S. Aubry, J. Chem. Phys. **62**, 3217 (1975); T. Schneider

and E. Stoll, Phys. Rev. Lett. **35**, 296 (1975); T. R. Koehler and P. A. Lee (unpublished).

⁵For example, K. A. Müller, N. S. Dalal, and W. Berlinger, Phys. Rev. Lett. **36**, 1504 (1976); R. A. Cowley, J. D. Axe, and M. Iizumi, Phys. Rev. Lett. **36**, 806 (1976).

⁶A. R. Bishop, E. Domany, and J. A. Krumhansl, Ferroelectrics (to be published).

⁷We are indebted to J. F. Currie for assistance in developing suitable computer programs.

⁸T. R. Koehler, A. R. Bishop, J. A. Krumhansl, and J. R. Schrieffer, Solid State Commun. **17**, 1515 (1975).

⁹The continuum approximation (15) was found elsewhere (see Ref. 8) to be an excellent representation of the discrete lattice wall solution in the displacive limit,

and even for $C/|A|$ as small as unity (see also Ref. 16).

¹⁰More rigorously, a full variation in result (21) is called for as discussed earlier in Sec. III.

¹¹For example, I. S. Gradshteyn and I. M. Ryzhik, *Table of Integrals, Series and Products*, 4th ed. (Academic, New York, 1965), p. 496.

¹²For a recent discussion of classical (one-dimensional) solitary wave behavior in the presence of various types of perturbation, see M. B. Fogel, S. E. Trullinger,

A. R. Bishop, and J. A. Krumhansl, *Phys. Rev. Lett.* **36**, 1411 (1976), and to be published.

¹³For example, T. Schneider, H. Beck, and E. Stoll, *Phys. Rev. B* **13**, 1123 (1976).

¹⁴See R. F. Dashen, B. Hasslacher, and A. Neveu, *Phys. Rev. D* **11**, 3424 (1975).

¹⁵A. Luther (unpublished).

¹⁶J. F. Currie, S. E. Trullinger, and A. R. Bishop (unpublished).